(1)

OFFICE OF NAVAL RESEARCH

Contract N00014-82K-0612

Task No. NR 627-838

TECHNICAL REPORT NO. 51

Electrochemical Investigations or Electronically Conductive Polymers. VI. Mechanism of the Redox Reactions for the Electronically Conductive Form of Polypyrrole

by

Zhihua Cai and Charles R. Martin

Prepared for publication

in

Journal of Electroanalytical Society

Department of Chemistry
Colorado State University
Ft. Collins, CO 80523

August 2, 1990

UNCLASSIFIED
SECURITY CLASSIFICATION OF THIS PAGE

REPORT DOCUMENTATION PAGE

Form Approved
OMB No. 0704-0188

1a. REPORT SECURITY CLASSIFICATION UNCLASSIFIED	1b. RESTRICTIVE MARKINGS
2a. SECURITY CLASSIFICATION AUTHORITY	3. DISTRIBUTION / AVAILABILITY OF REPORT APPROVED FOR DISTRIBUTION, DISTRIBUTION UNLIMITED.
2b. DECLASSIFICATION / DOWNGRADING SCHEDULE	
4. PERFORMING ORGANIZATION REPORT NUMBER(S) ONR TECHNICAL REPORT # 51	5. MONITORING ORGANIZATION REPORT NUMBER(S)
6a. NAME OF PERFORMING ORGANIZATION Dr. Charles R. Martin Department of Chemistry 6b. OFFICE SYMBOL (If applicable)	7a. NAME OF MONITORING ORGANIZATION Office of Naval Research
6c. ADDRESS (City, State, and ZIP Code) Colorado State University Ft. Collins, CO 80523	7b. ADDRESS (City, State, and ZIP Code) 800 North Quincy Street Arlington, VA 22217
8a. NAME OF FUNDING / SPONSORING ORGANIZATION Office of Naval Research 8b. OFFICE SYMBOL (If applicable)	9. PROCUREMENT INSTRUMENT IDENTIFICATION NUMBER Contract # N00014-82K-0612
8c. ADDRESS (City, State, and ZIP Code) 800 North Quincy Street Arlington, VA 22217	10. SOURCE OF FUNDING NUMBERS PROGRAM ELEMENT NO. / PROJECT NO. / TASK NO / WORK UNIT ACCESSION NO
11. TITLE (Include Security Classification) Electrochemical Investigations or Electronically Conductive Polymers VI. Mechanism of the Redox Reactions for the Electronically Conductive Form of Polypyrrole	
12. PERSONAL AUTHOR(S) Zhihua Cai and Charles R. Martin	
13a. TYPE OF REPORT Technical 13b. TIME COVERED FROM _____ TO _____	14. DATE OF REPORT (Year, Month, Day) (90, 08, 02) Aug. 2, 1990 15. PAGE COUNT
16. SUPPLEMENTARY NOTATION	
17. COSATI CODES FIELD / GROUP / SUB-GROUP	18. SUBJECT TERMS (~~Continue on reverse if necessary and identify by block number~~) polypyrrole, conductive polymers, insulator/conductor, transition

19. ABSTRACT (Continue on reverse if necessary and identify by block number)

A small amplitude current-step method has been developed to study redox reactions of polypyrrole at high doping levels (equilibrium potentials between 0.1 and 0.6 V vs. SCE). The polymer is an electronic conductor in this potential window. It has been rigorously proven that both the oxidation and reduction processes of polypyrrole films are purely capacitive in this potential region. The effect of external electrolyte concentration on the film resistance and capacitance was studied. The results suggest that the film ionic conductivity is determined by the concentration of excess free electrolyte inside the film. Charge balancing anions do not contribute to the ionic conductivity. It was also found that the morphology of polypyrrole films is uniform through out the film thickness. Finally, we present here a simple heuristic model for redox reactions of conductive polymers.

20. DISTRIBUTION / AVAILABILITY OF ABSTRACT ☒ UNCLASSIFIED/UNLIMITED ☐ SAME AS RPT ☐ DTIC USERS	21. ABSTRACT SECURITY CLASSIFICATION UNCLASSIFIED
22a. NAME OF RESPONSIBLE INDIVIDUAL Dr. Robert Nowak	22b. TELEPHONE (Include Area Code) (202) 696-4410 22c. OFFICE SYMBOL

DD Form 1473, JUN 86 *Previous editions are obsolete.*

SECURITY CLASSIFICATION OF THIS PAGE

UNCLASSIFIED

ONR Tech Report #51
J. Electroanal. Chem. Accepted

ELECTROCHEMICAL INVESTIGATIONS OF ELECTRONICALLY CONDUCTIVE POLYMERS. VI.

Mechanism of the Redox Reactions for the Electronically Conductive Form of Polypyrrole

Zhihua Cai[a] and Charles R. Martin[a,b]

Department of Chemistry

Texas A&M University

College Station, TX 77843

polypyrrole, ~~conductive~~ conductive polymers, insulator/conductor transition

[a] Present address:
Department of Chemistry
Colorado State University
Fort Collins, CO 80523

[b] To whom correspondence should be addressed.

ABSTRACT

A small amplitude current-step method has been developed to study redox reactions of polypyrrole at high doping levels (equilibrium potentials between 0.1 and 0.6 V vs. SCE). The polymer is an electronic conductor in this potential window. It has been rigorously proven that both the oxidation and reduction processes of polypyrrole films are purely capacitive in this potential region. The effect of external electrolyte concentration on the film resistance and capacitance was studied. The results suggest that the film ionic conductivity is determined by the concentration of excess free electrolyte inside the film. Charge balancing anions do not contribute to the ionic conductivity. It was also found that the morphology of polypyrrole films is uniform through out the film thickness. Finally, we present here a simple heuristic model for redox reactions of conductive polymers.

INTRODUCTION

Electronically conductive polymers can be chemically or electrochemically "switched" between electronically insulating and electronically conductive states (1-3). This insulator/conductor transition plays an integral role in nearly all of the proposed applications of these materials (4-8). Numerous researchers, in a variety of different fields of science, are currently investigating this insulator/conductor switching process (3).

The insulator-to-conductor transition in electronically conductive polymers may be represented by

$$-[M]_y - + nX_s^- \text{ -------> } -[M^+X^-]_n-[M_{(y-n)}]- + ne^- \quad (1)$$

where M represents a monomer unit and X^- is an anion, initially present in a contacting solution phase. The neutral polymer on the left hand side of Equation 1 is the insulating form; the polycation on the right hand side is the conductive form. Equation 1 indicates that charge must be transported through the polymer phase during the insulator-to-conductor conversion process.

We have initiated a series of investigations aimed at exploring the rates and mechanisms of charge-transport in electronically conductive polymers (8-10). Our previous papers have focused on the electronically insulating form of polypyrrole (9,10). We have shown that charge-transport in insulating polypyrrole is diffusive and that the rate of charge-transport can be described by an apparent diffusion coefficient (9). Small

amplitude electrochemical methods were used in these investigations to insure that the polymer remained in the insulating state throughout the duration of the experiment (9-10).

We have since focused our attention on the electronically conductive form of polypyrrole. We have used a small amplitude current step method to investigate the mechanism and rate of charge-transport in the conductive form of this polymer. We have found that charge-transport in the polymer at potentials positive of the anodic peak (Figure 1) appears to be purely capacitive in nature. Models developed to describe charging of porous metal films can, therefore, be applied to this (highly oxidized) form of the polymer. The film capacitance and resistance can be obtained from such analyses. We report the results of these and related investigations of the electronically conductive form of polypyrrole, in this paper.

EXPERIMENTAL

Materials and Equipment. Tetraethylammonium tetrafluoroborate (Aldrich, 99%) was recrystallized twice from methanol (Baker Analyzed, 99.9 %) and dried in vacuo (100°C, 24 hrs). Pyrrole (Aldrich, 99%) was distilled twice, under N_2, immediately prior to use. Acetonitrile (UV grade, Burdick Jackson), and all other reagents, were used as received.

The electrochemical equipment has been described previously (9). Electrochemical experiments were conducted in conventional one-compartment glass cells, at 23±2°C, under a nitrogen

atmosphere. Platinum disk working electrodes were prepared by heat-sealing Pt wire (dia=1 mm, Alfa) into Kel-F cylinders. The electrodes were then polished as described previously (11).

A large diameter (6 mm) platinum disk electrode coated with a 1 μm-thick polypyrrole film was used as the counter electrode. This insured that the process depolarizing the counter electrode was always the opposite of the (polymer redox) process occurring at the working electrode. Thus, contamination of the solution by redox products from the counter electrode was eliminated. A conventional saturated calomel electrode (SCE) was used as the reference electrode. All potentials are reported verse SCE.

Film Deposition. Polymerization solutions were prepared in acetonitrile and were 0.5 M in pyrrole and 0.2 M in Et_4NBF_4. Polymerization was accomplished galvanostatically at a current density of 1.0 mA cm^{-2}. A typical potential-time transient associated with the polymerization of pyrrole is shown in Figure 2. Film thickness was controlled by varying the charge passed during the polymerization (9). A Tencor Alfa-step profilometer was used to measure film thickness.

After electrochemical polymerization, the film was removed from the monomer solution and rinsed with degassed 0.1 M Et_4NBF_4 (in acetonitrile). The polymer electrode was then immersed into an acetonitrile solution containing the desired concentration of this electrolyte. Prior to performing other electrochemical measurements, cyclic voltammetry was routinely used to asses the quality of the freshly-synthesized film. Typical voltammograms

for a 0.27 μm-thick polypyrrole film are shown is Figure 1. Voltammograms for films up to 3 μm in thickness were qualitatively similar.

Small Amplitude Current Step Experiment. After the preliminary voltammetric characterization (e.g. Figure 1), the polypyrrole film-coated electrode was equilibrated for ca. 10 min. at the desired initial potential, E_o. Initial potentials used ranged from 0.0 to 0.6 V vs. SCE. The polymer electrode was then switched to open circuit and a 40-ms current pulse was applied. The magnitude of the applied current density varied from 5 to 500 $\mu A\ cm^{-2}$; the overpotential arising from these small current pulses was always less than 60 mV. The resulting potential-time transients were recorded and analyzed using the finite porous electrode model developed by Posey and Morozumi (12).

Porous Electrode Model. The theory for galvanostatic charging of a semi-infinite porous electrode was first considered by Ksenzhek and Stender (14) and De Levie (15). Posey and Morozumi (12) developed analogous theory for porous electrodes of finite length. All of these models assume an idealized one-dimensional porous electrode (13); however, Candy et al. (16) have recently shown that the impedances of porous electrodes in which the pores are non-cylindrical, finite in length, and interconnected are very similar to impedances predicated by these one-dimensional porous electrode models.

According to Posey and Morozumi's theory (12), when a constant current, i_o, is applied to a porous electrode of finite

thickness, the change in electrode potential is described by

$$E(t) - E_o = i_0 R_s + \frac{i_o t}{C_f} + \frac{2 i_o R_f}{\pi^2} \int_{k=0}^{k=\infty} \frac{1}{k^2} [1 - \exp(\pi^2 k^2 t / t_o)] \qquad (2)$$

where $E(t)$ is the potential at time t, E_o is the equilibrium potential before application of the current pulse, R_s is the uncompensated solution resistance, R_f is the ionic resistance of the porous electrode, C_f is the capacitance of the electrode, and t_o is the time constant; $t_o = R_f C_f$ (17).

The potential time transient described by Equation 2 can be divided into two temporal regions. When t is less than about $t_o/3$, $E(t)$ is be described by (14)

$$E(t) - E_o = i_o R_s + 2 i_o \left(\frac{R_f t}{\pi C_f}\right)^{1/2} \qquad (3)$$

In contrast, when t is greater than ca. $t_o/2$, $E(t)$ varies linearly with time (12); the slope of this linear portion of the transient is given by (12)

$$\frac{dE(t)}{dt} = \frac{i_o}{C_f} \qquad (4)$$

The theoretical basis for this transition in temporal response of the finite porous electrode is discussed by Posey and Morozumi (12). By plotting the short time data as E(t) vs. $t^{1/2}$ (Equation 3) and the long time data as E(t) vs. t (Equation 4) both C_f and R_f can be evaluated from a single current step experiment.

RESULTS AND DISCUSSIONS

Applicability of the Posey/Morozumi Model to Electronically Conductive Polypyrrole. Figure 3 shows typical E(t) vs. t transients for current steps at a polypyrrole film; both cathodic and anodic transients for three different values of the initial applied potential (E_o) are shown. (Note, again, that all three E_o's are positive of the anodic peak (Figure 1)). The short time data for these transients are plotted as E(t) vs. $t^{1/2}$ (Equation 3) in Figure 4.

The data in Figures 3 and 4 show that the Posey/Morozumi finite porous electrode model can be applied to the electronically conductive form of polypyrrole. In agreement with Equation 3, the short time E(t) data are linearly related to $t^{1/2}$ (Figure 4) and, in agreement with Equation 4, the long time E(t) data vary linearly with t (Figure 3). Furthermore, the potential-time transient associated with a cathodic current step, is superimposable with the E(t)-t transient associated with the analogous anodic step (Figures 3 and 4); this is the expected behavior for purely capacitive charging/discharging of a porous metal electrode (12-16).

This agreement between the experimental data and the predictions of the porous electrode model is only observed at potentials positive of the anodic peak (Figure 1). At potentials negative of the peak (yet still in the electronically conductive potential regime (18)), deviations from the finite porous electrode model are observed. The electrochemical response of polypyrrole can, therefore, be divided into three potential regimes - 1. A highly oxidized (and electronically-conductive) regime (0.1 V to ca. 0.6 V), where the porous metal model applies. This regime is the subject of the current paper. 2. An intermediate oxidation level (yet still electronically conductive) regime (0.0 to -0.3 V vs. SCE). The porous metal electrode model is not applicable to this regime. Results of electrochemical investigations of polypyrrole in this potential window will be described in a future publication (19). 3. The electronically insulating regime. This regime was the subject of our previous papers (9,10).

As indicated above, the data in Figures 3 and 4 provide qualitative evidence for the applicability of the porous electrode model to the highly oxidized form of polypyrrole. A semiquantitative evaluation of the model can be obtained by comparing experimental and theoretically-predicted transition times. The R_f and C_f values obtained from the data in Figures 3 and 4 are shown in Tables I and II. (These Tables provide R_f and C_f data for various values of E_o and i_o; these data will be discussed in greater detail later in this paper). The time

constant, t_o (see Equation 2), can be calculated from these R_f and C_f data; $t_o = R_f C_f$. For example, a time constant of $t_o = 0.55$ sec is calculated from the data obtained at $E_o = 0.4$ V (Tables I and II).

The porous electrode theory predicts that E(t) will vary linearly with t (Equation 4) at times greater than $t_o/2$; therefore, for $t_o = 0.55$ sec, the theory predicts a transition to linear dependence at times greater than 0.27 sec. An experimental approximation of this transition time can be obtained by conducting least squares analyses on the experimental data. For example, least squares analysis of the E(t) vs. t data in Figure 3a over the temporal window from 0.4 sec to 1.2 sec yields a correlation coefficient of 0.999. This, indicates that the long time E(t) data do, indeed, show good linearity with time (Equation 4).

If the lower limit of the time window for the least squares analysis is dropped to 0.3 sec, the correlation coefficient is 0.998, again indicating good linearity. If however, the lower limit of the time window is dropped to 0.2 sec, the least squares analysis yields a correlation coefficient of 0.989 and if the lower limit of the time window is dropped to 0.1 sec, a correlation coefficient of 0.973 is obtained. These simple statistical analyses suggest that the experimental E(t) data becomes linearly related to t at times greater than 0.3 sec and that linearity is substantially degraded for times less than 0.2 sec. This experimentally-observed transition region 0.2 to 0.3

sec, compares well with the theoretically-predicted transition time of 0.27 sec.

Analogous statistical analyses can be conducted on the short time data. The porous metal theory predicts linear E(t) vs. $t^{1/2}$ behavior in the temporal region $0 < t < t_o/3$. Again, for an equilibrium potential of 0.4 V, the experimental data in Tables I and II yield a value of $t_o/3$ of 0.2 sec. Linear least squares analysis of the experimental E(t) vs $t^{1/2}$ data over the time window $0 < t < 0.1$ sec yields a correlation coefficient of 0.999, indicating that the short time E(t) data are, indeed, linear with $t^{1/2}$. If the least squares analysis is extended to an upper time limit of 0.2 sec, the correlation coefficient is also 0.999. At higher upper time limits, however, the correlation coefficient decreases (0.3 sec gives 0.994; 0.4 sec gives 0.987). These data indicate that, as predicted by the theory, E(t) vs. $t^{1/2}$ linearity is degraded at long times. The calculated (0.2 sec) and experimental transition times are, again, in good agreement.

The porous metal electrode model also predicts that both C_f and R_f should be independent of the magnitude of the current pulse (i_o). Tables I and II show that this is, indeed, the case. Finally, it is of interest to note that while R_f is independent of E_o (Table I, vide infra), C_f initially decreases with increasing E_o and then becomes constant at high values of E_o (Table II). Tanguy et al. observed an analogous trend in C_f from Ac impedance studies of polypyrrole film (20).

Mechanism of Ionic Conduction in Electronically Conductive Polypyrrole. Because the electronically conductive form of polypyrrole is a polycation, charge-balancing anions are present in the polymer phase (Equation 1). However, it is now generally accepted that excess electrolyte is also incorporated into the polymer phase (20,21). We have conducted a series of experiments aimed at ascertaining the fraction of ionic charge carried by this excess electrolyte and the fraction carried by the charge-balancing anions.

The number of charge-balancing anions present in the polymer film must be equal to the number of oxidized pyrrole monomer sites; this number can be approximated by measuring the area under a slow scan linear sweep voltammogram (22-24). Figure 1 shows voltammograms for polypyrrole films which were in contact with acetonitrile solutions containing 0.1, 0.05, and 0.01 M Et_4NBF_4. The number of moles of oxidized monomer sites (and thus the moles of charge-balancing anions) calculated from these voltammograms are 5.8$\pm$0.5 nmoles (0.1 M electrolyte), 5.7$\pm$ 0.4 nmoles (0.05 M electrolyte), and 5.5$\pm$0.4 nmoles(0.01 M electrolyte).

While the quantity of charge-balancing anions does not change with the concentration of electrolyte in the contacting solution phase, the film resistance is strongly dependent on the solution electrolyte concentration (Table III). The data in Table III show that the quantity of excess electrolyte partitioned into the polymer film increases with the

concentration of electrolyte in the contacting solution phase and that the Et_4N^+ and excess BF_4^- partitioned into the polymer contribute to ionic conduction in the film. Thus, from the point of view of ionic conduction, the film may be viewed as two parallel resistors - a resistor associated with the movement of the charge-balancing BF_4^-'s and a resistor associated with the movement of the Et_4N^+ and the excess BF_4^- present in the film.

According to the above model, the total resistance of the film (R_T) can be expressed as $1/R_T = 1/R_B + 1/R_E$ where R_B is the resistor corresponding to the movement of the charge balancing BF_4^-'s and R_E is the resistor corresponding to the movement of the excess electrolyte in the film. This equation can be rewritten as

$$L_T = L_B + L_E \qquad (5)$$

where the L's are the corresponding conductances in the film. The conductance associated with the excess electrolyte in the film, L_E, is given by (25)

$$L_E = 2M_{salt,f}\,(U_{+,f} + U_{-,f})\,FA/d \qquad (6)$$

where $M_{salt,f}$ is the concentration of excess electrolyte in the film, $U_{+,f}$ and $U_{-,f}$ are the mobilities of the excess Et_4N^+ and BF_4^- (respectively) in the film, A is the film area, and d is the film thickness.

Equation 6 can be rewritten

$$L_E = 2kM_{salt,s}\,(U_{+,f} + U_{-,f})\,FA/d \qquad (7)$$

where k is the partition coefficient for the electrolyte between the solution and polymer phases, and $M_{salt,s}$ is the concentration of electrolyte in the solution phase. Substitution of Equation 7 into Equation 5 gives

$$L_T = L_B + 2kM_{salt,s} (U_{+,f} + U_{-,f}) FA/d \quad (8)$$

According to Equation 8, if the partition coefficient, k, does not vary with the concentration of electrolyte in the solution phase, L_T will increase linearly with $M_{salt,s}$; the conductivity due to the charge-balancing BF_4^-'s (L_B) would then be the intercept in a plot of L_T vs. $M_{salt,s}$. It is, however, unlikely that k would be independent of the electrolyte concentration in solution because activity effects in both the solution and film phases have been ignored and because the film will ultimately saturate with electrolyte (i.e. the partition isotherm will appear langmuirian (26)). Extrapolation of the experimental L_T vs. $M_{salt,s}$ curve to $M_{salt,s} = 0$ will, nevertheless, provide L_B.

Figure 5 shows the experimental data plotted as per Equation 8; as expected, downward curvature is observed at high salt concentrations. Extrapolation of the experimental curve to zero shows, however, that the conductivity of the charge-balancing BF_4^-'s is vanishingly small. Thus, for solution electrolyte concentrations above ca. 0.05 M, ionic conduction in the film is accomplished almost exclusively by the excess electrolyte.

The low conductivity of the charge-balancing BF_4^-'s (relative to the excess electrolyte) could be attributable either to low

concentration or low mobility of these charge-balancing anions. Our previous investigations have shown that when the concentration of electrolyte in the contacting solution phase is 0.2 M, the concentration of the excess electrolyte in the polymer is about the same as the concentration of charge-balancing anions in the polymer (9). Therefore, the low conductivity of the charge-balancing BF_f^-'s is due to low mobility of these anions in the polymer phase. This low mobility is undoubtedly caused by strong electrostatic attraction to the fixed cationic sites on the polymer chain.

Dependence of Polymer Morphology on Film Thickness. In a previous publication, we suggested that electrochemically synthesized polypyrrole becomes more dense as the thickness of the nascent polymer layer increases (9). As a result, we proposed that thick films of polypyrrole are more dense than thin films of this polymer. The experiment described in this paper provides an avenue for exploring this putative densification effect (9).

Let us assume, for the moment, that thin films of polypyrrole are, indeed, less dense than thick films; this would mean that thin films are more porous than thick films and this, in turn, would make the resistivities of thin films higher than the resistivities of thick films. Table IV shows resistivities for various thicknesses of polypyrrole film. In contrast to the above analysis, resistivity is independent of film thickness.

Capacitance data can also be used to determine whether thin

films are more porous than thick films. Table V shows capacitance data (normalized for film thickness) for various polypyrrole films. If thin films are more porous, the thickness-normalized capacitances for the thin films would be higher than for the thick films. As was the case for the resistivity data (Table V), the normalized capacitance is independent of film thickness.

The data in Tables IV and V indicate that, in contrast to our earlier suggestion (9), the density of polypyrrole does not change with film thickness. This conclusion is corroborated by a recent investigation by Larry et al. who found that the concentration of counterions in polypyrrole is uniform throughout the film thickness (27).

Anisotropy in the Electronic Conductivity of Polypyrrole. Electronic conductivity in polypyrrole involves movements of positively charged carriers (28,29) and/or electrons (31,31) along polymer chains and hopping of these carriers between chains. Thus the electronic conduction process can be viewed as a series sum of two resistors - an intrachain transport resistor and an interchain hopping resistor. It is generally believed that the interchain hopping resistance is much greater than the intrachain transport resistance (28-32).

Electron diffraction data suggest that the polymer chains in electrochemically-synthesized polypyrrole lie parallel to the substrate electrode surface (33). If this is the case, conductance parallel to the film surface would involve fewer

interchain hopping events than conductance across the thickness of the polymer film. Thus, electrochemically-synthesized polypyrrole films should show higher conductivities along the film surface than across the film thickness. To test whether electrochemically-synthesized polypyrrole film shows such conduction anisotropy, we synthesized films with thicknesses of 36 and 72 μm and removed these films (intact) from the substrate electrode surfaces. The conductivity parallel to the film surface ($S_{||}$) was measured using a four-point method (34); the conductivity across the film thickness ($S_{\perp}$) was measured using a method developed in these laboratories (35).

$S_{||}$ and $S_{\perp}$ were 90 ± 8 ($\Omega^{-1}cm^{-1}$) and 0.25 ± 0.03 ($\Omega^{-1}cm^{-1}$), respectively, and were independent of film thickness. These data yield a conduction anisotropy ($S_{||}/S_{\perp}$) of 360. This large anisotropy indicates that, in agreement with the electron diffraction data (33), the polymer chains in electrochemically-synthesized polypyrrole do, indeed, lie parallel to the substrate electrode surface. Cuetko et al. (36) have also observed conduction anisotropy for polypyrrole film; their value ($S_{||}/S_{\perp}$ = 3.5) is two orders of magnitude smaller that the value obtained here. It is of interest to note, however, that Cvetko et al. investigated films which were much thicker than the films used here. This suggests that preferential ordering of the polymer chains parallel to the electrode surface is lost, or diminished, in very thick polypyrrole films.

CONCLUSIONS

We have shown that a current step method, initially developed for analyzing porous metal electrodes, can be applied to the highly oxidized form of the electronically conductive polymer polypyrrole. This model provides the capacitance and the ionic resistance of the polymer film and allows for investigations of the effects of such variables as equilibrium potential, film thickness, electrolyte concentration, electrolyte type, etc. on R_f and C_f. Pickup has recently described a potential step method which can provide analogous data (37). One advantage of the method described here is that the experimental data are not distorted by uncompensated solution resistance. Uncompensated resistance is a potential problem in the potential step method.

A Heuristic Model for Redox Reactions of Conductive Polymers. A recurrent question, regarding the voltammetry of conducting polymers, is - what fraction of the current observed is capacitive and what fraction is faradaic (9,10). For example, are the raising portions in the voltammograms shown in Figure 2 predominantly faradaic? Likewise, are the large, potential-independent, currents observed at potentials positive of the anodic peak predominantly capacitive? As pointed out in our previous paper, these questions are confounded by the fact that, on a molecular level, polymer "capacitive currents" result from the same process as polymer "faradaic currents" - extraction/injection of electrons from/into the polymer chain (9).

The experimental data obtained here, and in our other papers

on the mechanisms of charge-transport in conductive polymers (3,8-10,38,39), have suggested a model which resolves the "capacitive current" vs. "faradaic current" controversy. This model is, undoubtedly, overly simplified but is useful from a heuristic point of view. We present this simple heuristic model below. We use polypyrrole to illustrate this model; however this model should apply to all electronically conductive polymers.

As indicated earlier, our experimental data suggest that the redox chemistry of polypyrrole can be divided into three regimes. These regimes are defined by the applied potential of the substrate electrode. The first is a low potential regime where the polymer is an electronic insulator. The oxidation of this reduced form of polypyrrole appear diffusional (9,10). The second regime occurs at high potentials (vide supra), where the polymer is an electronic conductor. As indicated in this paper, both oxidation and reduction of polypyrrole appear capacitive in this potential regime. The final regime occurs at intermediate potentials. The polymer is an electronic conductor but neither the diffusional nor capacitive models apply (19).

These three regimes form the basis of our model. Let us begin by reviewing the difference between a faradaic and a capacitive current - A faradaic current involves charge-transport <u>across an interface</u>; capacitive currents involve charge storage <u>at an interface</u>. We believe that the controversy of whether a current is capacitive or faradaic in a conductive polymer can be addressed by posing the question - <u>Where is the relevant</u>

interface? The answer to this question is different for each of the three potential regimes discussed above.

Consider, first the electronically insulating form of polypyrrole. Where is the relevant interface when this form of the polymer is oxidized. While there are two interfaces, the electrode/polymer interface is the most important. This is a nonohmic interface between an electronic conductor and an electroactive electronic insulator. Such electrode/electroactive polymer interfaces are analogous to electrode/electroactive solution interfaces and conventional faradaic electron transfer occurs across these interfaces (40). Charge is also stored at such interfaces. Indeed, in our previous papers we measured the capacitance of the double layer at the Pt/polypyrrole interface (9,10).

The bottom line is that oxidation of the insulating form of polypyrrole is initially completely analogous to oxidation of a redox polymer (40). There is faradaic electron transfer across the electrode/polymer interface and charge storage at this interface. This conclusion is in complete accord with the relevant experimental data (9,10).

Consider, next, the completely oxidized, electronically conductive form of polypyrrole. This form is highly porous; Miller's data suggest a porosity of ca. 40 percent (40). This pore space is filled with an electrolyte phase which is similar to the external electrolyte (9). The simplest way to explain the high porosity is to assume that the individual polymer chains are

immersed within the internal electrolyte phase (Figure 6; the key point is that large aggregates of chains in which the interiors of the aggregates are isolated from the internal electrolyte are not possible because of the very high porosity). Finally, note that these individual chains are electronic conductors (i.e. they are molecular wires).

Now, where is the relevant interface? There is an interface between the substrate electrode and the base of each molecular wire; however, this is now an ohmic interface, quite different from the electronic conductor/electronic insulator interface encountered in the previous example. From an electrochemical point of view, the important interface is now the interface between the molecular wires and the internal electrolyte phase.

In contrast to the redox polymer case, charge is not transported across the molecular wire/internal electrolyte interface. Rather, charge is pulled out of the molecular wire (across an ohmic junction) and a counterion (from the internal electrolyte phase) is bound at the surface of this wire. Thus, polymer redox reactions in this high potential regime resemble purely capacitive processes. Furthermore the surface area associated with these capacitive processes is very large. These conclusions are in complete accord with the data presented here and in prior investigations (20,24).

It is important to point out that a substantial amount of charge is passed via this purely capacitive mechanism. For example, the anodic charge under the flat part of the

voltammetric wave, at potentials positive of the anodic peak, (see e.g. Figure 2) can account for as much as 40 % of the total anodic charge passed during a voltammetric experiment. Thus, while electrochemists usually try to minimize capacitive currents in voltammetric experiments, such currents are always significant for electronically conductive polymers.

So far our model has explained the purely diffusional nature for the redox reaction when the polymer is in its insulating form and the purely capacitive nature when the polymer is in its highly oxidized form. What about the intermediate potential regime? Again, the electrochemical data in this regime follow neither the capacitive nor diffusional models. We believe that the unique electrochemical response in this regime arises because there are both conductive and insulating regions within the polymer film.

The most simple model for this intermediate potential regime is of a redox polymer (the insulating, reduced, regions of the polypyrrole) which has molecular wires (the conductive, oxidized, regions of the polymer) running through it. Note first that the presence of the molecular wires will insure that the film will (in the net) be electronically conductive. This is in agreement with the observation that polypyrrole becomes conductive at very low levels of oxidation (9). However, the question - <u>where is the relevant interface</u> - becomes very complicated.

For the molecular wires, the interface of importance is (again) the interface between the wire and the surrounding

electronically-insulating (polypyrrole) phase. As discussed above charge is stored at this molecular wire/electronic insulator interface. In addition, however, if an oxidation process is occurring, electrons are being transported across this interface from the surrounding reduced polypyrrole region (vide infra).

Likewise, electrons are being transported across the interface between the substrate electrode and the reduced polymer regions. For both the molecular wires and the substrate electrode, these electrons are collected via a diffusive mechanism (9) from the reduced polymer regions. This process creates more molecular wires and less insulating polypyrrole (i.e. it oxidizes the polypyrrole).

The bottom line is that in this intermediate potential window both the capacitive and diffusive mechanisms are operative and an intermediate electrochemical response is obtained. This conclusion is in complete accord with the observed experimental data (19,20,24). We hope that this simple, but diagnostic, heuristic model will aid in the development of more sophisticated models for the redox reactions of electronically conductive polymers.

REFERENCES

1. C. K. Chiang, M. A. Druy, S. C. Gau, A. J. Heeger, E. J. Louis, A. G., MacDiarmid, Y. W. Park, and H. Shirakawa, J. Am. Chem. Soc., **100**, 1013 (1978).

2. A. F. Diaz, K. K. Kanazawa, and G. P. Gardini, J. Chem. Soc. Chem. Commun., 1979: 635 (1979).

3. C. R. Martin, L. S. Van Dyke, "Mass and Charge Transport in Electromically Conductive Polymers." in R. W. Murray Ed., Molecular Design on Electrode Surface, Wiley, in press.

4. P. Burgemayer, and R. W. Murray, J. Am. Chem. Soc., **104**, 6139 (1982).

5. H. S. White, G. P. Kittlesen, and M. S. Wright, J. Phys. Chem. 89, 5133 (1985).

6. N. S. Sundaresan, S. Basak, M. Pomeraztz, and J. R. Reynolds, J. Chem. Soc., Chem. Commun., **621** (1987).

7. A. Mohamadi, Q. Inagnas, and I. Lustrom, J. Electrochem, Soc., **133**, 947 (1986).

8. C. R. Martin, M.J. Tierney, I. F. Cheng, L. S. Van Dyke, Z. Cai, J. R. McBride, and C. J. Brumlik, Polymer Preprint, **30**, 424 (1989).

9. R. M. Penner, L. S. Van Dyke, and C. R. Martin, J. Phys. Chem., **92**, 5274 (1988).

10. R. M. Penner, and C. R. Martin, J. Phys. Chem., **93**, 984 (1989).

11. C. R. Martin and K. A. Dollard, J. Electroanal. Chem. **159**, 127 (1983).

12. F. A. Posey and T. Morozumi, J. Electrochem. Soc., **113**, 176 (1966).

13. De Levie, in Advances in Electrochemistry and Electrochemical Engineering, P. Delahay, and C. W. Tobias, Eds., Interscience: New York, 1967, Vol. 1.

14. O. S. Ksenzhek and V. V. Stender, Zhur. Fiz. Khim; **31**, 117 (1957).

15. R. De Levie, Electrochim. Acta, **8**, 751 (1963).

16. J. Candy, P. Fouiloux, M. Keddam, and H. Takenouti, Electrochim. Acta, **26**, 1029 (1981).

17. A. J. Bard, and L. R. Faulker, Electrochemical Methods Theory and Applications, Wiley, New York, 1980; pp. 55,56.

18. B. J. Feldman, P. Burgmayer, and R. W. Murray, J. Am. Chem. Soc., **107**, 872 (1985).

19. Z. Cai and C. R. Martin, in preparation.

20. J. Tanguy, N. Mermilloid, and M. Hocklet, Synth. Met., **18**, 7 (1987).

21. Q.Z. Zho, C. J. Kolaskie, and L. L. Miller, J. Electroanal. Chem., **223**, 238 (1987).

22. A. F. Diaz, J. I. Castillo, J. A. Logan, and W. Y. Lee, J. Electroanal. Chem. **129**, 115 (1981).

23. R. A. Bull, F. Fan, and A. J. Bard, J. Electrochem. Soc., **129**, 1011 (1982).

24. S. W. Felderg, J. Am. Chem. Soc., **106**, 4671 (1984).

25. A. J. Bard, and L. R. Faukler, Electrochemical Methods Theory and Applications, Wiley, New York, 1980; p.123.

26. W. H. Atkins, Physical Chemistry; W.H. Freeman and Company: New York, 1986, pp. 777,778.

27. S. C. Larry, G. G. Komphlin, and W. J. pietro, J. Phys. Chem., **92**, 12 (1988).

28. R. R. Chance, J. L. Bredas, and R. Silbey, Phys. Rev. B., **29**, 4491 (1984).

29. R. R. Chance, D.S. Bourdreauz, J. L. Bredas, and R. Silbey, in "Handbook of Conducting Polymers, Volume **2**,:, T. J. Skotheim, Ed., p. 915, Marcel Dekker, New York (1986).

30. R. H. Baughman and L. W. Shacklette, Synthetic Metals, **17**, 173 (1987).

31. C. R. Fincher, M. Ozaki, M. Tanaka, D. Peebles, L. Lanchlan, A. J. Heeger, and A. G. Macdiarmid, Phys. Rev. B. **20**, 1589 (1979).

32. M. Tanaka, A. Watanabe, H. Fujimoto, and J. Tanaka, Mol. Cryst. Liq. Cryst., **82**, 277 (1982).

33. R. H. Geiss, G. B. Street, W. Volksen,and J. Economy, IBM J. Rev. Dev. **27**, 321 (1983).

34. J. R. Reynolds, Ph.D dissertation, U. of Massachusetts, Amherst, MA(1984).

35. Z. Cai, C. Liu, and C. R. Martin, J. Electrochem. Soc. 136, 3356 (1989).

36. B. F. Cvetko, M. P. Brungs, R. P. Burford, and M. Skullas-Kazacos, J. Appl. Electrochem., **17**, 1198 (1987).

37. H. Mao and P.G. Pickup, J. Phys. Chem., **93**, 6480, (1989).

38. L.S. Van Dyke and C.R. Martin, Langmuir 6, 1118 (1990).

39. L.S. Van Dyke and C.R. Martin, Synth. Met. In press.

40. C.E.D. Chidsey and R.W. Murray, Science (Washington, D.C.), 231, 25 (1986).

41. D. L. Miller, Dissertation, Texas A&M University, 1990.

Acknowledgements. This work was supported by the Air Force Office of Scientific Research the NASA Johnson Space Center, and the Office of Naval Research.

Table I Film Resistance (in kOhms)[a] at Different Initial Film Potentials Measured by Both Anodic and Cathodic Current Steps.[b]

E_{eq} (V)	i_o (μA cm^{-2})					
	0.64		1.28		1.92	
	Anodic	Cathodic	Anodic	Cathodic	Anodic	Cathodic
0.1	2.9±0.2	2.8±0.2	0.9±0.2	3.0±0.2	2.9±0.2	2.9±0.2
0.2	2.7±0.2	2.7±0.2	2.7±0.2	2.7±0.2	2.7±0.2	2.8±0.2
0.3	2.6±0.2	2.6±0.2	2.6±0.2	2.6±0.2	2.6±0.2	2.6±0.2
0.4	2.4±0.2	2.5±0.2	2.5±0.2	2.5±0.2	2.4±0.2	2.4±0.2
0.5	2.6±0.2	2.6±0.2	2.6±0.2	2.5±0.2	2.6±0.2	2.6±0.2
0.6	2.7+0.2	2.7±0.2	2.7±0.2	2.6±0.2	2.8±0.2	2.7±0.2

[a] Each datum represents the average of four measurements.

[b] The film was 1.32 μm-thick and was in contact with 0.2 M Et_4NBF_4/MeCN solution.

Table II. Film Capacitances (in μF)[a] at Different Film Initial Potentials Measured by Anodic and Cathodic Current Steps.[b]

E_{eq} (V)	i_o($\mu A\ cm^{-2}$)					
	0.64		1.28		1.92	
	Anodic	Cathodic	Anodic	Cathodic	Anodic	Cathodic
0.1	326±15	324±15	318±15	325±15	312±15	311±15
0.2	262±15	258±152	258±15	257±15	268±15	258±152
0.3	246±10	238±15	241±10	235±15	244±15	235±15
0.4	225±10	220±15	233±15	228±15	228±10	219±15
0.5	225±10	215±15	226±10	213±13	230±10	210±15
0.6	240±10	212±15	235±10	211±152	241±10	209±15

[a] Each datum represents the average of four measurements.

[b] The film was 1.32 um-thick and was in contact with 0.2 M Et_4NBF_4/MeCN solution.

Table III. Dependence of Film Capacitance[a] and Resistance[a] on the Concentration of Et_4NBF_4 in the Contacting Solution Phase.[b]

Electrolyte Conc. (M)	0.4	0.2	0.05	0.01
C_f (μF)	103±2	104±3	100±2	97±2
R_f (kΩ)	0.71±0.04	1.14±0.05	2.8±0.1	18.2±0.6

[a] Each datum is the average of five measurements.

[b] Film thickness was 0.53 μm.

Table IV Dependence of Film Resistivity on Film Thickness[a].

Film thickness (μm)	0.53	0.79	1.32	2.64
Film resistivities[b] (KΩ cm)	170$\pm$7	157$\pm$9	173$\pm$14	181$\pm$13

[a] E_o = 0.2 V

[b] Each datum is the average of four or five measurements.

Table V Dependence of the Film Capacitance (Normalized for Film Thickness) on the Film Thickness.[a]

Film thickness (μm)	0.13	0.53	0.79	1.32	2.64
Normalized Capacitance[b] (Farads/μm)	230±30	200±20	200±10	210±9	220±10

[a] E_o = 0.2 V.

[b] Each datum is the average of four or five measurements.

Figure Caption

Fig. 1. Cyclic voltammograms for a 1.32 μm-thick polypyrrole film in solutions containing various concentrations of Et_4NBF_4. Initial potential = -0.8 V; scan rate = 10 mV/s.

Fig. 2. Typical potential-time transient from the galvanostatic preparation of a 1.32 μm-thick polypyrrole film. Polymerization conditions: current density = 1.0 $mAcm^{-2}$, solution = 0.5 M pyrrole/0.2 M Et_4NBF_4/MeCN.

Fig. 3. Overpotential-time transients for current-step experiments initiated at various initial potentials. Initial potentials were a. 0.4 V; b. 0.2 V; d. 0.1 V. Supporting electrolyte = 0.2 M Et_4NBF_4; current step amplitude = 1.25 $mAcm^{-2}$; film as per Figure 1.

Fig. 4. Plots of overpotential vs $t^{1/2}$ from the transients in Fig. 3.

Fig. 5. Plot of film conductance vs. external electrolyte concentration. Film thickness = 0.53 μm; E_o = 0.2 V.

Fig. 6. Simple heuristic model for the morphology of completely oxidized polypyrrole.

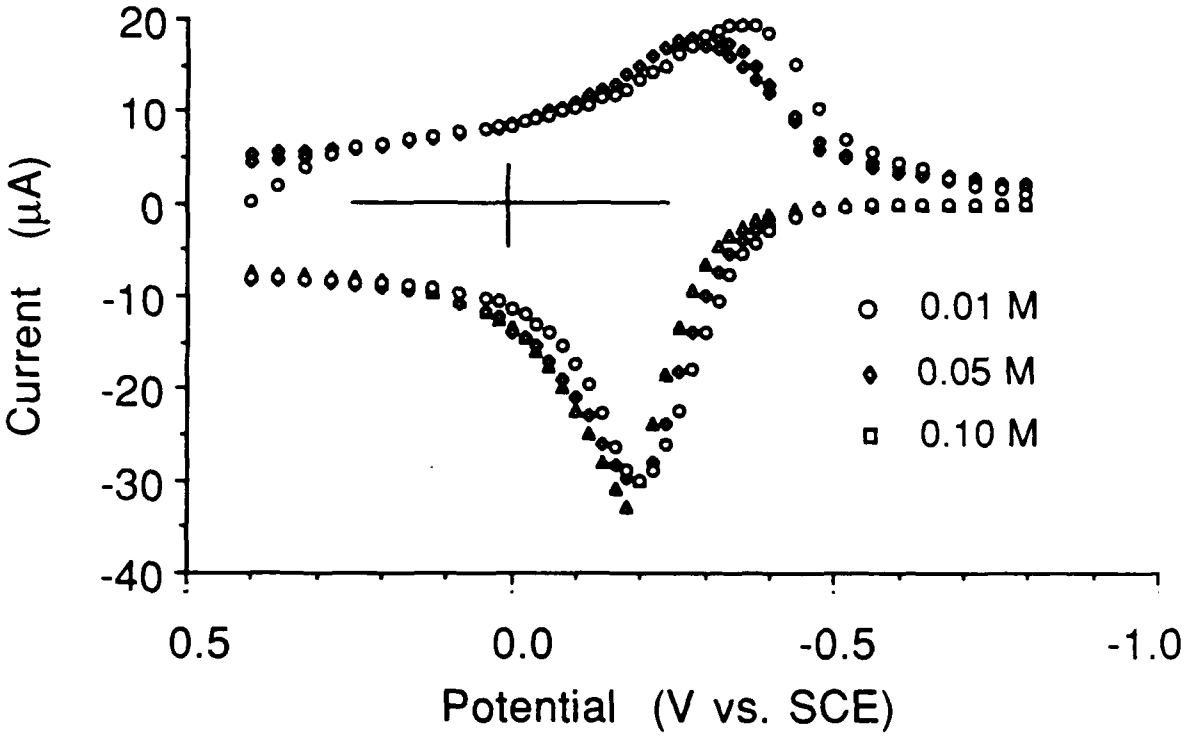
20
10
0
-10
-20
-30
-40
Current (μA)
0.01 M
0.05 M
0.10 M
0.5
0.0
-0.5
-1.0
Potential (V vs. SCE)

Figure 1

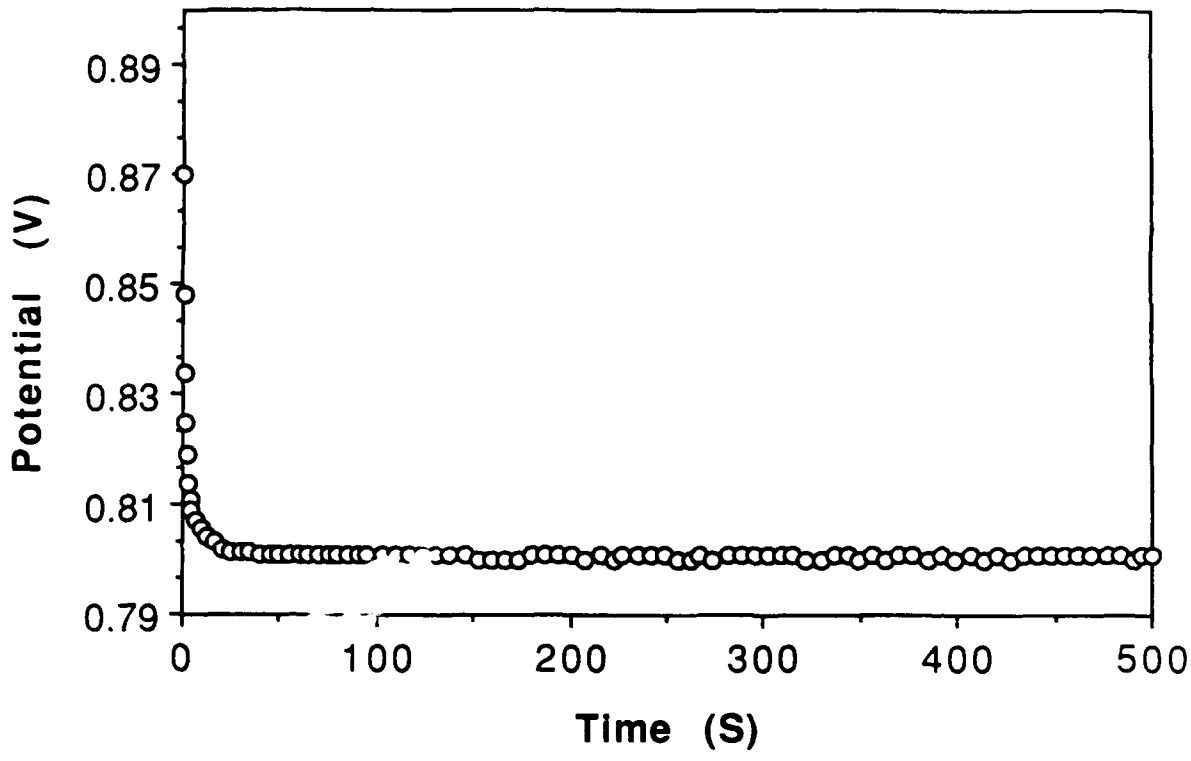

Figure 2

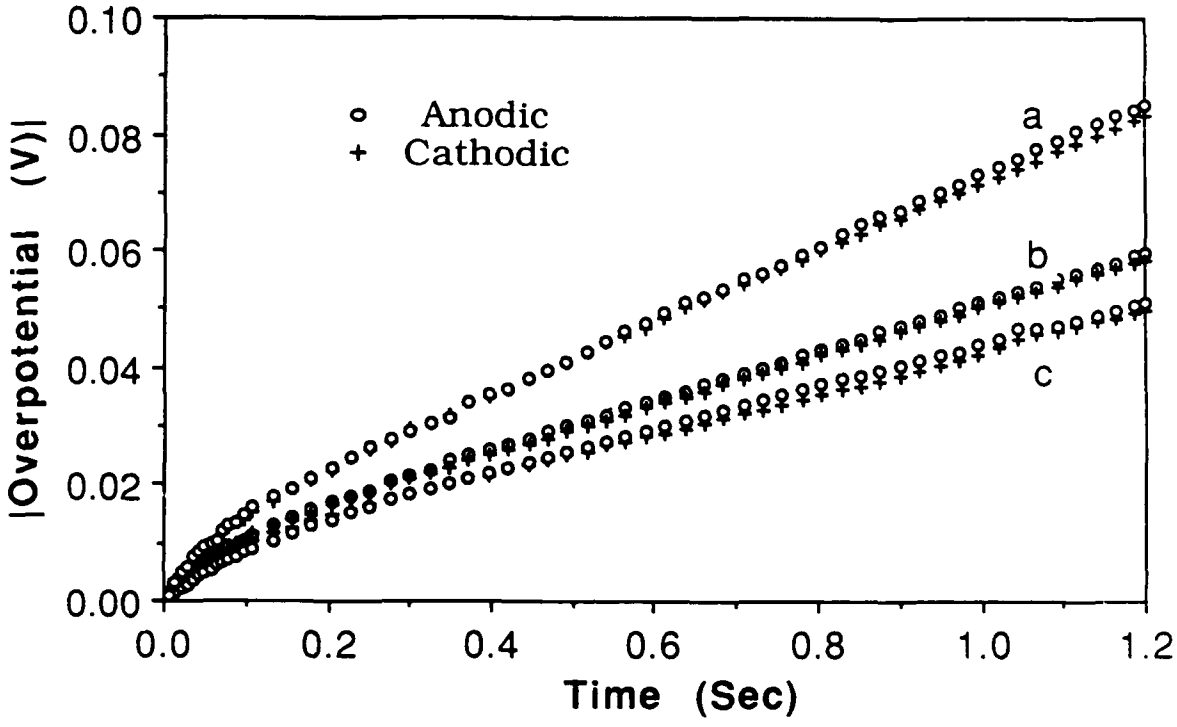
0.10
0.08
0.06
0.04
0.02
0.00
|Overpotential (V)|
Anodic
Cathodic
a
b
c
0.0
0.2
0.4
0.6
0.8
1.0
1.2
Time (Sec)

Figure 3

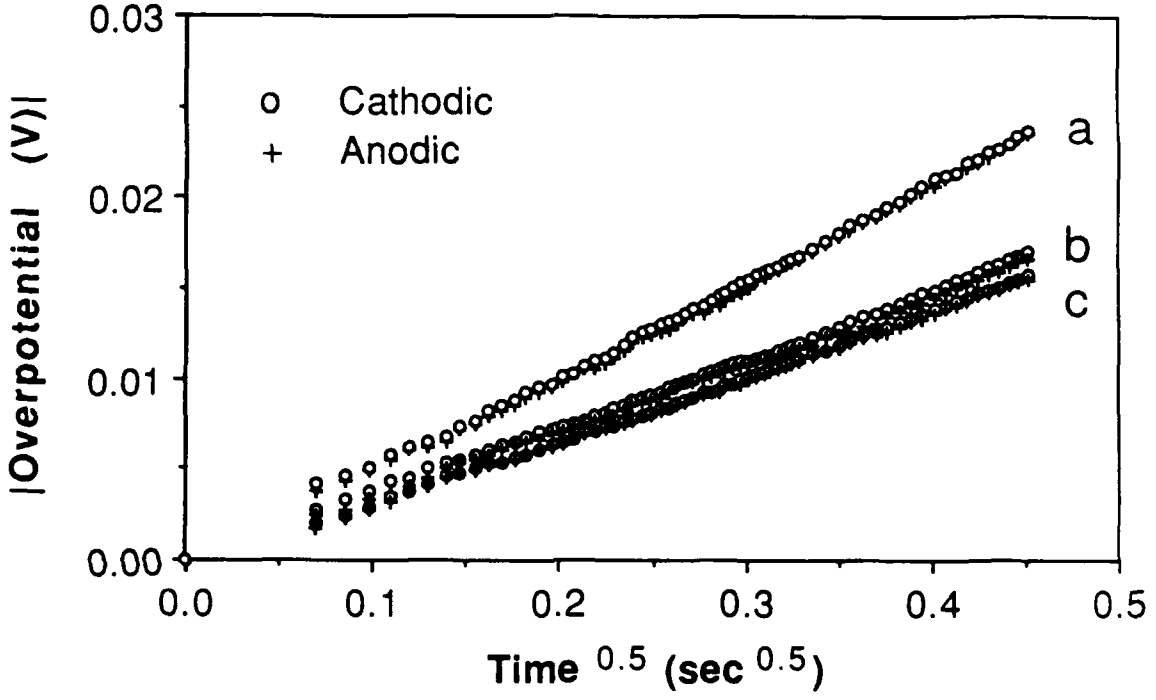
0.03
0.02
0.01
0.00
|Overpotential (V)|
o Cathodic
+ Anodic
a
b
c
0.0
0.1
0.2
0.3
0.4
0.5
Time 0.5 (sec 0.5)

Figure 4

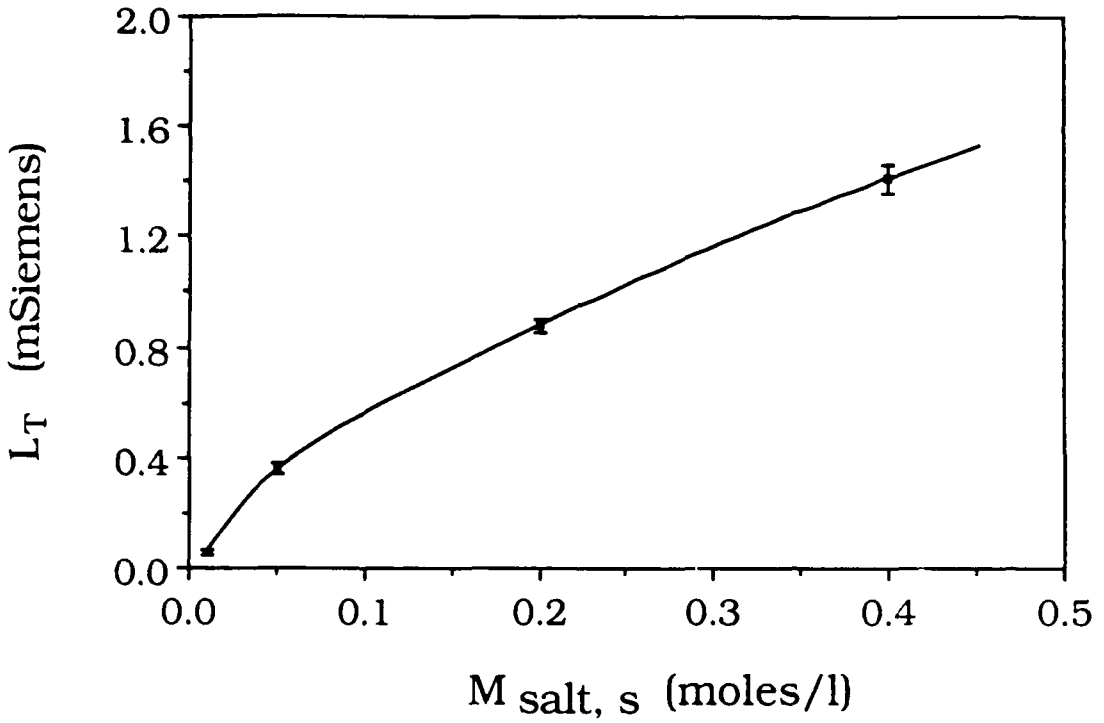

Figure 5

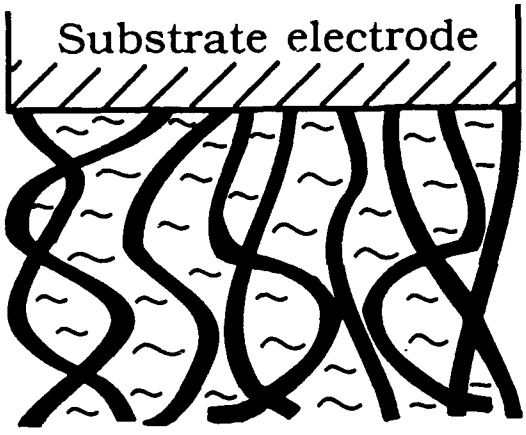

External electrolyte phase

= Individual polypyrrole chain (i.e. molecular wire)

= Internal electrolyte phase

Fig. 6